

The metallicity and star formation activity of long gamma-ray burst hosts for $z < 3$: insights from the Illustris simulation.

L. A. Bignone^{1*}, P. B. Tissera^{1,2}, L. J. Pellizza⁴

¹*Instituto de Astronomía y Física del Espacio (IAFE, CONICET-UBA), C.C. 67 Suc. 28, C1428ZAA Ciudad de Buenos Aires, Argentina.*

²*Departamento de Ciencias Físicas, Universidad Andres Bello, Av. Republica 220, Santiago, Chile.*

⁴*Instituto Argentino de Radioastronomía (CCT-La Plata, CONICET; CICPBA), C.C. No. 5, 1894, Villa Elisa, Argentina.*

Accepted XXX. Received YYY; in original form ZZZ

ABSTRACT

We study the properties of long gamma-ray bursts (LGRBs) using a large scale hydrodynamical cosmological simulation, the Illustris simulation. We determine the LGRB host populations under different thresholds for the LGRB progenitor metallicities, according to the collapsar model. We compare the simulated sample of LGRBs hosts with recent, largely unbiased, host samples: BAT6 and SHOALS. We find that at $z < 1$ simulated hosts follow the mass-metallicity relation and the fundamental metallicity relation simultaneously, but with a paucity of high-metallicity hosts, in accordance with observations. We also find a clear increment in the mean stellar mass of LGRB hosts and their SFR with redshift up to $z < 3$ on account of the metallicity dependence of progenitors. We explore the possible origin of LGRBs in metal rich galaxies, and find that the intrinsic metallicity dispersion in galaxies could explain their presence. LGRB hosts present a tighter correlation between galaxy metallicity and internal metallicity dispersion compared to normal star forming galaxies. We find that the Illustris simulations favours the existence of a metallicity threshold for LGRB progenitors in the range $0.3 - 0.6 Z_{\odot}$.

Key words:

gamma-ray burst: general – galaxies: abundances, evolution – methods: numerical

1 INTRODUCTION

The study of the galaxy population hosting long gamma-ray Bursts (LGRBs) provides a fundamental source of information to constrain the nature of LGRB progenitors. For example, the link between LGRBs and the death of massive stars (Hjorth et al. 2003, 2012) is supported by a clear preference of LGRBs to be found in star-forming galaxies (Le Flocc’h et al. 2003; Savaglio et al. 2009). As tracer of star formation, LGRBs offer unique advantages since their intrinsic high luminosity makes them detectable up to very high redshifts ($z > 6$, Tanvir et al. 2012; Basa et al. 2012; Salvaterra 2015). This makes them promising tools to study star formation in faint and distant galaxies (e.g. Kistler et al. 2008; Robertson & Ellis 2012; Greiner et al. 2015), a problem that would be otherwise difficult to tackle using traditional star-forming galaxy surveys that can be

affected by redshift incompleteness, magnitude limits and dust extinction.

Evidence suggests that star formation is not the only factor regulating the production of LGRBs. If that were the case, the LGRB population would sample star-forming galaxies with a probability proportional to the galaxy star formation rate (SFR). However, LGRB hosts show a preference for bluer and less luminous galaxies (Le Flocc’h et al. 2003), and crucially, with a lower metallicity than typical star forming galaxies (Stanek et al. 2006; Modjaz et al. 2008; Savaglio et al. 2009; Graham & Fruchter 2013; Jimenez & Piran 2013). The existence of other factors which might influence the production of LGRBs is still a matter of debate (Heuvel et al. 2013), but metallicity is often cited as a major regulator of the LGRB rate (e.g. Wolf & Podsiadlowski 2007; Kocevski et al. 2009; Trenti et al. 2015).

Low metallicity is often predicted by core-collapse progenitor models which require the retention of the angular momentum of the central core to launch the jet in

* E-mail: lbignone@iafe.uba.ar

the first place (Woodsley 1993; MacFadyen & Woodsley 1999; Izzard et al. 2004). Single progenitor models predict very low metal progenitors in the range $Z < 0.1 - 0.3 Z_{\odot}$ (Woodsley & Heger 2006), while binary progenitor models favour a less stringent metallicity dependence (Izzard et al. 2004; Fryer & Heger 2005; Podsiadlowski et al. 2010). Hence, the metallicity of LGRB hosts is an important observable to distinguish between these two families of models.

Observationally, there has been significant improvements in the construction of LGRB host samples. Early samples suffered from both heterogeneous observations of galaxy properties and the probable presence of selection biases (Le Flocc'h et al. 2003; Fruchter et al. 2006; Savaglio et al. 2009; Levesque et al. 2010; Svensson et al. 2010; Mannucci et al. 2011; Graham & Fruchter 2013; Perley et al. 2013; Hunt et al. 2014). Hosts samples selected from optical afterglows, which are subjected to dust extinction, tend to under-represent the more metal-rich and more massive hosts that are typically related to heavily obscured or dark LGRBs (Fynbo et al. 2009; Perley et al. 2013).

Current samples are instead constructed from the X-ray LGRB emission, which is largely unaffected by dust attenuation, and follow a carefully chosen set of selection criteria. Among these, are the BAT6 (Salvaterra et al. 2012), TOUGH (Hjorth et al. 2012) and SHOALS (Perley et al. 2016a) samples. Also redshift completeness has been greatly improved, reaching values close to 90 percent for the 69 objects in the TOUGH sample, ≥ 90 percent for the 58 objects in the BAT6 sample and 68 percent for the larger SHOALS sample composed of 119 objects.

For these new host samples, detailed and homogeneous follow up observations have allowed a clearer picture to emerge, at least, at low redshift ($z \leq 1.5$). Vergani et al. (2015) found a strong deficiency of higher stellar mass galaxies in the BAT6 sample at low redshift, as shown by their K-band luminosity. These hosts were further studied by Japelj et al. (2016) who analysed the detected nebular emission lines to measure the dust extinction, SFR and nebular metallicity. They found that the high mass deficiency is accompanied by a paucity of metal-rich LGRB hosts. Similar results were found for the SHOALS sample by Perley et al. (2016b) who studied the irac $3.6 \mu m$ luminosity which can be readily correlated with stellar mass. They found that the host stellar mass increases with redshift, and that such trend could be explained by a model in which the LGRB rate is uniform with respect to metallicity below solar but drops by about an order of magnitude in metal-rich galaxies. Similarly, Schulze et al. (2015) found that hosts in the TOUGH sample favour lower UV luminosities, specially at low redshifts and that the UV brighter hosts are located in the $1 < z < 3$ range. These results, reproduced by independent and largely unbiased samples suggest that, at low redshift, the LGRBs are indeed produced preferentially in low-metallicity environments.

Some of these studies predict higher metallicities thresholds (e.g. Perley et al. 2016b) than the ones favoured by single progenitor models. It is still unclear to what extent mean host metallicities are representative of LGRB progenitor metallicities. It could be still possible for low-metallicity star formation to occur in globally high-metallicity hosts either due to metallicity gradients, accretion of poorly en-

rich material or metallicity inhomogeneity in the interstellar medium (ISM) of galaxies (Niino 2011).

The metallicity dependence of LGRB host galaxies have been studied using different models and approximations, most of them based on the hypothesis that the host metallicity is traced by the metallicity of the stellar progenitor or vice-versa. For example, Wolf & Podsiadlowski (2007) studied the efficiency of producing LGRBs assuming that LGRB hosts followed the luminosity-metallicity relation of star-forming galaxies. They found that if a metallicity cut-off existed for the formation of the LGRBs, it was in the order of solar metallicity. Similarly, Trenti et al. (2015) predicted the luminosities, stellar masses, and metallicities of LGRB hosts assuming that they followed the mass-metallicity relationship (MZR) derived by Maiolino et al. (2008) and that LGRBs could be produced through both a metallicity dependent and independent channels. They found a moderate metallicity bias, where most LGRBs (80%) are in very low metallicity environments produced by collapsars and the remaining 20% are produced by the metallicity independent channel.

Alternatively, theoretical approaches using both semi-analytic models of galaxy formation (Lapi et al. 2008; Campisi et al. 2009; Chisari et al. 2010) and cosmological hydrodynamical simulations (Nuza et al. 2007; Niino 2011; Salvaterra 2015) provide a more consistent description of the chemical properties of the local ISM and of the global galaxy. In particular, considering that galaxy formation is a highly non-linear process, and that the computation of LGRB host properties assuming a metallicity bias depends strongly on a detailed knowledge of galaxy assembly, cosmic star-formation and chemical evolution of the ISM, cosmological hydrodynamical simulations (Katz & Gunn 1991; Navarro & White 1993; Mosconi et al. 2001; Springel & Hernquist 2003; Scannapieco et al. 2005, 2006) are specially suitable for this task since they provide a self-consistent description of these processes within a cosmological context.

Early studies using hydrodynamical simulation yielded results consistent with the existence of a metallicity threshold for the triggering of LGRBs events (Courty et al. 2004; Nuza et al. 2007). These simulations implemented simple subgrid physics and described small cosmological volumes, which limited galaxy statistics and made difficult the study of rare, more massive, galaxies, while lower resolutions made the results of low mass galaxies more uncertain. Current hydrodynamic simulations have dramatically improved this situation thanks to larger volumes and more sophisticated models. In particular, the cosmological hydrodynamical simulation so-called Illustris (Vogelsberger et al. 2014a,b) attempts to reproduce the galaxy population using state-of-the-art star formation, supernovae and AGN feedback mechanisms. The Illustris simulation reproduces many observed quantities, among them, the stellar mass distribution of galaxies, their morphology, and gas content (Vogelsberger et al. 2014b; Genel et al. 2014). The big advantage of the Illustris simulation is its large cosmological volume, $\sim 100^3 \text{ Mpc}^3$. Hence, for the first time it is possible to construct a simulated LGRB host galaxy sample covering different environments and allowing a more suitable comparison with observations. Previous studies used small volumes or resorted to semi-analytical techniques (e.g.

Courty et al. 2004; Nuza et al. 2007; Campisi et al. 2009; Artale et al. 2011; Salvaterra et al. 2013).

In this work, for the first time, we propose to study the metallicity dependant model using a cosmological significant LGRB galaxy sample selected from the the state-of-the-art hydrodynamic cosmological Illustris simulation. We compare the SFR, sSFR, metallicity and mass distributions of the LGRB hosts predicted by the Illustris simulation to the complete and largely unbiased host samples BAT6 and SHOALS. Furthermore, the nature of the hydrodynamical simulation allows us to study simultaneously the metallicity of the LGRB hosts and the metallicity dependence that acts upon LGRB progenitors. Therefore we also aim at studying the origin of high-metallicity host galaxies.

The paper is organized as follows. Section 2 describes the simulations and the LGRB progenitor model. In Section 3 the properties of the LGRB host galaxies are analysed and compared to observations. Section 4 discusses the relation between the metallicity dispersion of the galaxy hosts and the metallicity of the LGRB progenitor. In Section 5 we describe the mass distribution of the simulated LGRB hosts in a cosmological context. In Conclusions, the main results are summarized.

2 NUMERICAL MODELS

2.1 Overview of the Illustris Simulation

The Illustris project (Vogelsberger et al. 2014a; Genel et al. 2014) consists of a series of large-scale hydrodynamical cosmological simulations with periodic box 106.5 Mpc a side, computed using the quasi-Lagrangian AREPO code (Springel 2010). The Illustris project adopted the following set of cosmological parameters: $\Omega_m = 0.2726$, $\Omega_\Lambda = 0.7274$, $\Omega_b = 0.0456$, $\sigma_8 = 0.809$, $n_s = 0.963$ and $h = 0.704$, which are consistent with the Wilkinson Microwave Anisotropy Probe (WMAP)-9 measurements (Hinshaw et al. 2013).

In our work we use the highest resolution simulation (Illustris-1, hereafter Illustris simulation). This simulation has a dark mass resolution of $6.26 \times 10^6 M_\odot$, and an initial baryonic gas mass resolution of $1.26 \times 10^6 M_\odot$. The number of initial resolution elements for both baryonic and dark matter is 1820^3 . The gravitational softening scale is 710 pc at $z = 0$, while the smallest gas cells extend to 48 pc. At $z = 0$ well-resolved galaxies (i.e. those with more than 500 stellar particles) have minimum stellar masses in the range $10^{8-9} M_\odot$, which is typical of LGRB hosts.

The Illustris simulations follows the gravitational and dynamical evolution of galaxies within a cosmological context, including primordial and metal line radiative cooling with self-shielding corrections, stellar evolution with associated mass loss and chemical enrichment of the interstellar medium (ISM), stellar wind feedback driven by SNe, super-massive black hole (SMBH) growth by accretion and mergers; and active galactic nuclei (AGN) feedback with radio, quasar and radiative modes (Vogelsberger et al. 2013; Marinacci et al. 2014; Torrey et al. 2014). The Illustris simulation is able to reproduce reasonably well many of the key observable trends in the local Universe, with some discrepancies related to the stellar ages of low mass galaxies and the quenching of massive galaxies (Vogelsberger et al. 2014b).

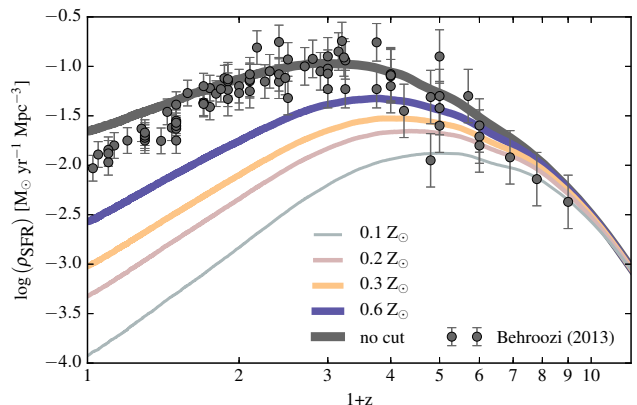


Figure 1. The cosmic star formation rate density for the Illustris simulation (thick grey line) and estimations using stellar populations with metallicity below a given metallicity threshold: 0.1 (green line), 0.2 (brown line), 0.3 (yellow line) and 0.6 (blue line) Z_\odot . For comparison, the observations compiled by Behroozi et al. (2013) (circles) are included.

The dark matter halos were identified using the standard friends-of-friends (FoF) algorithm (Davis et al. 1985) with linking length of 0.2 times the mean particle separation and a minimum number of 32 particles. Other particle types (stellar particles, gas cells, SMBH particles) were assigned to the FoF group of the closest DM particle. Finally, gravitationally bound substructures within the FoF groups were identified using the SUBFIND algorithm (Springel et al. 2001; Dolag et al. 2009). We refer to these subhalos, when mentioning galaxies in the simulation. Each galaxy has a well defined stellar mass based on the particles which are bound to it. Throughout the rest of the paper, we refer to this mass as the stellar mass of a galaxy.

Our sample of simulated galaxies is selected to have a minimum stellar mass of $10^8 M_\odot$. From this galaxies we build up the LGRB host galaxy sample which is the largest simulated sample of LGRB host galaxies hitherto analysed in this kind of simulation. At $z = 0$, they constitute 78,608 galaxies located in different environments in the 106.5 Mpc a side cubic volume.

2.2 LGRB population synthesis model

If we assume that the stellar progenitors of LGRBs are massive stars with a minimum mass M_{\min} , then the LGRB rate should follow the star formation rate in a perfectly unbiased way. In this case the intrinsic cosmic LGRB rate can be related to the cosmic star formation rate density ($\dot{\rho}_{\text{SFR}}(z)$) as

$$\Psi_{\text{LGRB}}(z) = \frac{\int_{M_{\min}}^{100 M_\odot} \psi(m) dm}{\int_{0.1 M_\odot}^{100 M_\odot} m \psi(m) dm} \dot{\rho}_{\text{SFR}}(z), \quad (1)$$

where ψ is the initial mass function (Chabrier 2003, in the case of the Illustris simulation) with lower and upper stellar mass limits of $0.1 M_\odot$ and $100 M_\odot$, respectively. Within this scenario, the production of LGRBs is not significantly delayed with respect to the star formation events that created their progenitor stars, since they are massive, short-lived objects.

Fig. 1 shows the cosmic star formation rate density for the Illustris simulation compared to observations (Behroozi et al. 2013). The predicted $\dot{\rho}_{\text{SFR}}(z)$ is in good agreement with observations at intermediate and high redshifts but presents some tension at lower redshifts where the simulated star formation is higher than expected. The excess of star formation appears to be related to insufficient AGN feedback in lower stellar-mass galaxies (see Vogelsberger et al. 2014b; Genel et al. 2014, for a more detailed discussion) that contribute the most star formation at lower redshift. Higher stellar-mass galaxies at low redshift are effectively quenched by AGN feedback from central SMBHs.

A preference of LGRBs for low-metallicity progenitors can be easily included by considering only the contribution to the $\dot{\rho}_{\text{SFR}}(z)$ from young stars with a metallicity below a selected threshold (Z_{th}). In Fig 1 we show the $\dot{\rho}_{\text{SFR}}(z)$ estimated by adopting $Z_{\text{th}} = 0.1, 0.2, 0.3$ and $0.6 Z_{\odot}$. As can be seen, the peak of the relation shifts to higher redshift for lower metallicity thresholds. The intrinsic LGRB rate for a given Z_{th} is then

$$\Psi_{\text{LGRB}}(z, Z_{\text{th}}) = \Sigma(z, Z_{\text{th}})\Psi_{\text{LGRB}}(z), \quad (2)$$

where $\Sigma(z, Z_{\text{th}})$ is the fraction of newborn stellar mass with metallicities below Z_{th} . $\Sigma(z, Z_{\text{th}})$ depends on the baryonic physics implemented in the simulations or analytical models. In hydrodynamical simulations, such as Illustris, stellar populations are represented by particles with an assigned mass, age and metallicity. Therefore, when determining $\Sigma(z, Z_{\text{th}})$ we take into account only individual stellar particles with age < 10 Myr and metallicity below Z_{th} .

3 SIMULATED LGRB HOST GALAXIES

Following previous works (Campisi et al. 2009; Chisari et al. 2010; Artale et al. 2011), we assign each galaxy a probability of being considered an LGRB host. This probability is then used as a weight to compute the distribution of the physical properties of the synthetic host galaxies sample such as stellar mass, SFR, metallicity, etc. These weighted distributions of observable synthetic parameters can be compared to the corresponding observational distributions. For a galaxy to be considered a host, at least one LGRB must be detected by a high-energy satellite. Then, the galaxy itself must be detected. A significant advantage of the state-of-the-art LGRB galaxy samples, such as BAT6, TOUGH and SHOALS, is that they select hosts exclusively based on the properties of the X-ray LGRB emission and favourable observing conditions. As consequence, biases related to the detection of the host galaxy are largely eliminated. This suggests to take the host probability p_{host} proportional to the contribution of each galaxy to the observed LGRB rate. As all distribution will be computed at constant redshift, all cosmological related terms, as well as factors related to detector sensitivity, become constant. Therefore p_{host} can be further simplified taking it proportional to the intrinsic number of LGRBs produced in a given galaxy (g),

$$N(g, Z_{\text{th}}) = m_*(g, Z_{\text{th}}) \frac{\int_{M_{\text{min}}}^{100 M_{\odot}} \psi(m) dm}{\int_{0.1 M_{\odot}}^{100 M_{\odot}} m \psi(m) dm}, \quad (3)$$

where $m_*(g, Z_{\text{th}})$ is the total stellar mass of young stars (age < 10 Myr) with metallicity below Z_{th} .

3.1 Mass-metallicity relation

Considering that the metallicity is assumed to play a significant role in the triggering of LGRBs, the MZR of the LGRB host galaxies in relation to the whole galaxy population is an important aspect to analyse. In order to perform direct comparisons to observations of galactic gas-phase metallicities, we obtain from the simulation the mass-weighted average metallicity of the gas cells bound to each galaxy, but restricted to cells which are star forming. This places an emphasis on star-forming gas, mimicking observational metallicity estimates from nebular emission lines. Particularly, the Illustris project does not track individual chemical elements, rather, they provide the metallicity as the ratio of the total gas mass of elements heavier than He to the total galaxy gas mass. In order to compare our results to observations, we convert the provided values to a metallicity expressed in terms of the oxygen-to-hydrogen abundance ratio ($12 + \log(\text{O}/\text{H})$). To do so a primordial solar metal mass fraction value of $Z_{\odot} = 0.0127$ (Wiersma et al. 2009) and a solar oxygen abundance value of $12 + \log(\text{O}/\text{H}) = 8.69$ (Asplund et al. 2009) are assumed.

In Fig. 2 we compare the simulated MZR of the synthetic LGRB host sample to the MZR of observed LGRB hosts obtained by Japelj et al. (2016) for the BAT6 sample, limited to $0.3 < z < 1$. The mean redshift of this observational sample is ~ 0.7 , which coincides with the redshift of the simulated hosts displayed in this figure. Here we show only the host metallicities in the Maiolino et al. (2008) calibration, but analogous conclusions can be extracted from the Kobulnicky & Kewley (2004) calibration.

Also, we compare our results to the MZR of field galaxies using the parametrised analytical model of Maiolino et al. (2008). As pointed out by Japelj et al. (2016), at sub-solar metallicities, observed LGRB hosts appear fairly consistent with the field MZR relation. In particular, there are no signs of a systematic offsets towards values below the relation as was the case in previous studies (Mannucci et al. 2011; Campisi et al. 2011). This could have been produced by incomplete samples (e.g. Levesque et al. 2010). Instead, there is a clear paucity of high stellar-mass hosts above the solar metallicity.

If no metallicity cut-off for LGRB progenitors is assumed, the MZR of simulated hosts appears very different from observations. In that case, high metallicity galaxies have the largest probability of hosting LGRBs, due to their high SFRs. Only a strong metallicity threshold can compensate for this effect. The lower panels of Fig 2 shows the results of considering $Z_{\text{th}} = 0.3, 0.2$ and $0.1 Z_{\odot}$. As can be seen, a significant shift towards lower metallicity hosts can be appreciated.

It is worth pointing out that the MZR of the Illustris simulation provides a good match to the field star-forming galaxies MZR but with some differences, as results evident in the first panel of Fig 2. First, the simulated relation presents a steeper slope than observations, with a significant number of high stellar-mass galaxies appearing above the Maiolino et al. (2008) relation, while lower stellar-mass ones appear below it. Secondly, a substantial population of

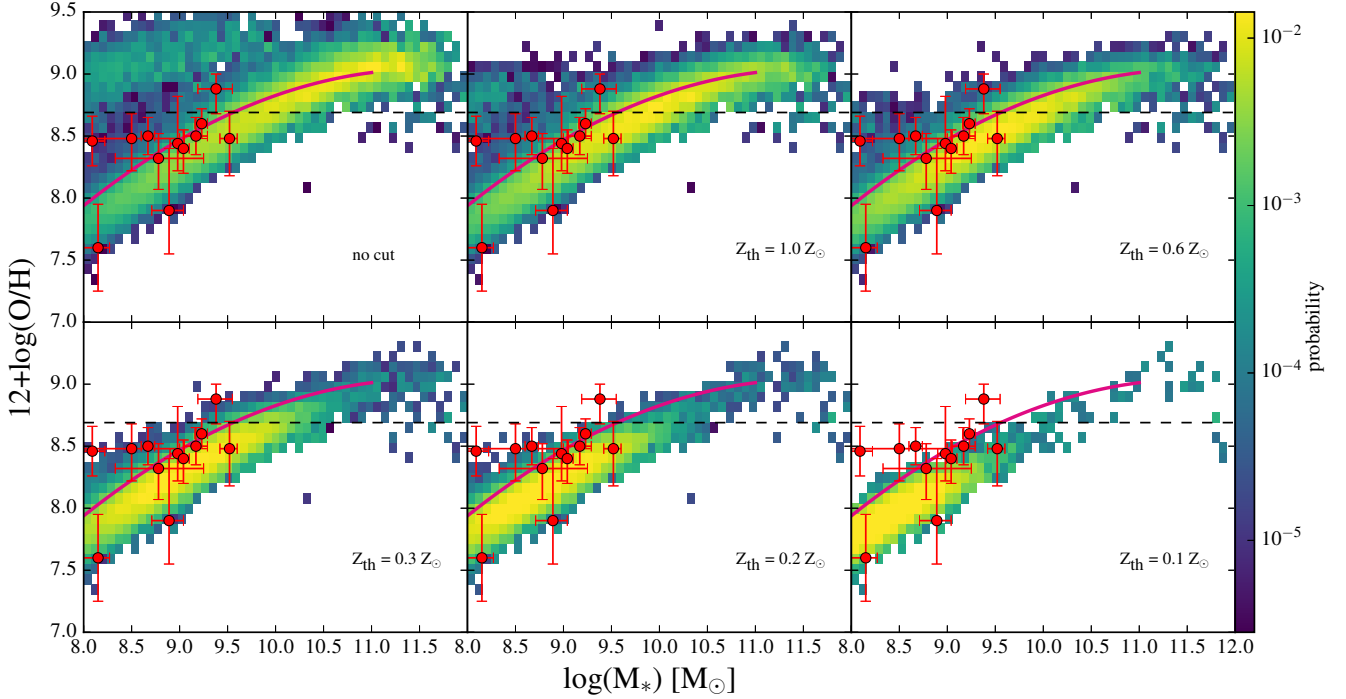


Figure 2. Mass-metallicity relation for host galaxies in the Illustris simulation at $z = 0.7$. In each panel the bins are weighted by the probability of hosting an LGRB according to a different metallicity threshold. For comparison to observations we show the Japelj et al. (2016) MZR for the BAT6 sample in the M08 calibration (points). Also shown is the MZR of field galaxies using the parametrised analytical model of Maiolino et al. (2008) (solid lines)

low stellar-mass, high-metallicity galaxies are found which do not have an observational counterpart. These issues appear to be related to the SN feedback model adopted in the Illustris simulation as discussed in detail by Torrey et al. (2014). The origin of the steeper relation is suggested to be due to metal low retention efficiency of low stellar-mass galaxies due to galactic winds with large mass loading factor. But the opposite seems to be the case for a certain subpopulation of low, stellar-mass galaxies where metal retention is too high. Regardless of these issues, the conclusion drawn in the previous paragraphs remains robust in the sense that LGRB hosts appear to indeed follow the MZR intrinsic to the simulation and that a metallicity threshold is required for most of the higher metallicity galaxies to be excluded. Also, we notice that a comparatively high metallicity threshold ($Z_{\text{th}} \sim 1$) is enough to discard the artificial low-mass, high-metallicity galaxies as potential LGRB hosts. Therefore, our conclusions are not affected by their presence in the simulation.

It should also be mentioned that the accurate determination of metallicities is a challenging task and that several methods exist for this purpose. Unfortunately, not all methods are reliable for all redshift and metallicity ranges. In particular, strong-line methods are used for galaxies too faint, distant or metal-rich for their metallicities to be measured by the preferred electron temperature (T_e) method (Pagel et al. 1979; Alloin et al. 1979). Strong-line methods have to be calibrated against oxygen abundances previously determined either empirically, via the T_e method (e.g. Pettini & Pagel 2004; Pilyugin & Grebel 2016), or theoretically, via photoionization models (e.g. McGaugh 1991;

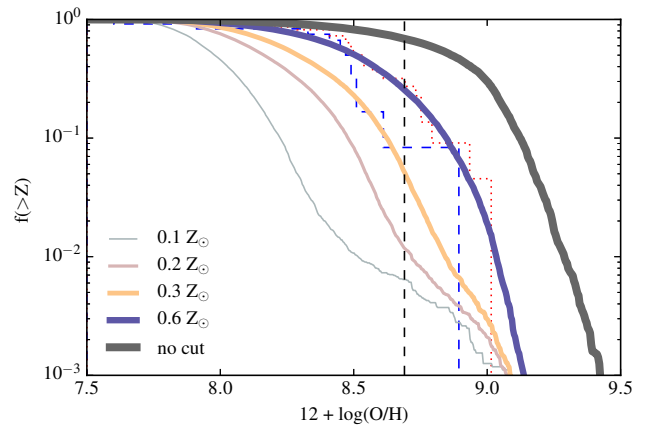


Figure 3. Normalized cumulative distribution of galaxies as a function of the metallicity of simulated LGRB hosts at $z = 0.7$ for models with no metallicity threshold as well as those with $Z_{\text{th}} = 0.1, 0.2, 0.3, 0.6 Z_{\odot}$. The black vertical line represents the solar oxygen abundance value of 8.69. The cumulative distributions of BAT6 (blue dashed line) and VLT/X-Shooter sub-samples (dotted, red line) at $z < 1$ are included for comparison.

Kobulnicky & Kewley 2004; Dopita et al. 2016). Different calibrations can result in large discrepancies of up to ~ 0.7 dex (Moustakas et al. 2010; Kewley & Ellison 2008). Recently, Curti et al. (2017) derived a new set of fully empirical calibrations for strong-line diagnostics. They find that in the high-metallicity regime ($12 + \log(O/H) > 8.2$) the metallicities determined by the T_e method are significantly

lower than those predicted by the photoionization models used by [Maiolino et al. \(2008\)](#) in their calibration. This suggests that at least part of the discrepancies found in the MZR of the Illustris simulation could be attributed to the calibration method and that, if [Maiolino et al. \(2008\)](#) metallicities were revised downwards, this would result in a better agreement between observations and the simulation as far as metallicities are concerned.

In Fig 3 the normalized cumulative number distribution of simulated LGRB hosts as a function of the mean metallicity of the host are shown at $z = 0.7$. The distributions are estimated for different metallicity thresholds. It is clear that observed LGRB hosts are in disagreement with the model with no metallicity threshold. The best match seems to be in the range $Z_{\text{th}} = 0.3 - 0.6 Z_{\odot}$. A Kolmogorov–Smirnov (K-S) test results in a p-value¹ of 0.024 and 0.059 for $Z_{\text{th}} = 0.3 Z_{\odot}$ and $Z_{\text{th}} = 0.6 Z_{\odot}$, respectively. For lower metallicities, the model with $Z_{\text{th}} = 0.6 Z_{\odot}$ indeed appears to be consistent with observations, but the BAT6 metallicity fraction of LGRB host with $Z_{\text{th}} > 8.5$ drops quickly to values more consistent with the model corresponding to $Z_{\text{th}} = 0.3 Z_{\odot}$.

We also compare our results to the metallicity distribution derived by [Krühler et al. \(2015\)](#) for their VLT/X-Shooter emission-line spectroscopy sample of LGRB host galaxies. The advantages of this sample are the large number of galaxies (96 galaxies) and a uniform set of measured properties including systemic redshifts, SFRs, visual attenuations (A_V) and oxygen abundances. Although their GRB selection criteria was not as carefully designed to avoid biases as the previously mentioned samples, this sample does include a significant number of dark and dusty LGRB hosts. In our analysis we limit the VLT/X-Shooter to $z < 1$ (22 galaxies) so it can be fairly compared to both the BAT6 sample and to the Illustris simulation at $z = 0.7$. The model with $Z_{\text{th}} = 0.6 Z_{\odot}$ appears to be a good match to these observations with a K-S test resulting in a p-value of 0.279. The drop for high metallicity hosts is weaker than in the case of BAT6, perhaps due to the larger sample size. Alternatively, the larger proportion of higher metallicity hosts could be related to the higher than average number of dusty hosts included in the VLT/X-Shooter sample.

In both BAT6 and the VLT/X-Shooter sample, the number of hosts with a metallicity above solar is relatively small compared to what is expected for typical star forming galaxies. From the sub-sample of $z < 1$ hosts with metallicity measurements, [Krühler et al. \(2015\)](#) derived a fraction of 24 ± 10 per cent of supra-solar metallicity hosts in the VLT/X-Shooter sample, while [Japelj et al. \(2016\)](#) found a fraction of 16_{-8}^{+16} for the BAT6 sample in the same redshift range. Our model with $Z_{\text{th}} = 0.6 Z_{\odot}$ presents a similar fraction of ~ 25 per cent of LGRB hosts with average metallicities above solar. The fraction of supra-solar metallicity hosts falls sharply when considering stricter thresholds, reaching less than 5 per cent for $Z_{\text{th}} = 0.3 Z_{\odot}$.

¹ Throughout this work we use the common definition that the p-value of the K-S test is the probability that the maximum absolute deviation between the cumulative distributions of both samples exceeds the observed value under the assumption that the null hypothesis, i.e. that both samples are drawn from the same distribution, is true.

3.2 Fundamental metallicity relation

The fundamental metallicity relation (FMR) is a tight correlation between stellar mass, metallicity and SFR that has been shown to be followed by star-forming galaxies at least up to $z < 2.5$ ([Mannucci et al. 2010](#)). [Mannucci et al. \(2011\)](#) compared the FMR of field galaxies with $M_* > 10^{8.3} M_{\odot}$ to the metallicity properties of a small sample of LGRB hosts at $z < 1$. They found that LGRB host galaxies follow the FMR within errors. The same result was found by [Japelj et al. \(2016\)](#) in the case of the $z < 1$ BAT6 sample. In Fig 4 we show the FMR of host galaxies in the Illustris simulation at $z = 0.7$ for different metallicity thresholds. For comparison we also show the BAT6 sample as well as the parametrised analytical expression of [Mannucci et al. \(2010\)](#) (dashed lines) and [Mannucci et al. \(2011\)](#) (solid lines).

The results are similar to the ones found for the MZR, the simulation follows a similar trend compared to the observed FMR, although slightly shifted towards lower metallicity values. The model with no metallicity threshold generates a large excess of high metallicity hosts which largely disappears when considering a more strict Z_{th} . However, it is clear that, in agreement with observations, the predicted LGRB hosts including a metallicity threshold follow the general FMR but with a higher proportion of low metallicity hosts.

It is important to point out that the host sample used by [Mannucci et al. \(2011\)](#), while following the FMR of star-forming galaxies, also presents a systematic offset towards lower metallicities with respect to the MZR of field galaxies. Previous works have used the results of [Mannucci et al. \(2011\)](#) to argue against a metallicity threshold, they claim that the apparent scarcity of high metallicity hosts could be explained by a higher than average SFR. That conclusion was reached for example by [Campisi et al. \(2011\)](#) who used N-body simulations combined with semi-analytical models of galaxy formation to study LGRB under different metallicity thresholds. These results are in tension with both the BAT6 sample and the Illustris simulation, which predict that hosts follow both the MZR and FMR simultaneously, regardless of the metallicity threshold. It is likely that the [Mannucci et al. \(2011\)](#) sample suffered from selection biases, that have largely been corrected in the BAT6 sample.

3.3 Star Formation Rate

Star-forming galaxies have been shown to follow the so called star formation main sequence (SFMS) at low ($z < 1$, [Brinchmann et al. 2004](#); [Salim et al. 2007](#)) and high ($z > 1$, [Daddi et al. 2007](#)) redshift. The sequence is an almost linear relation between the SFR and M_* , with a normalization that is observed to increase from $z=0$ to 2, around the same redshift where the $\dot{\rho}_{\text{SFR}}(z)$ also peaks.

Figure 5 shows the SFMS for the simulated hosts at $z = 0.7$ compared to the BAT6 sample. As pointed out by [Japelj et al. \(2016\)](#), the SFR of the BAT6 sample increases with stellar mass as expected. We also show for comparison the median SFMS relation derived by [Whitaker et al. \(2012\)](#), dashed red line) and [Whitaker et al. \(2014\)](#), solid blue line) where they extended the relation down to lower stellar masses ($M_* > 10^{8.4} M_{\odot}$). As can be seen, while BAT6 hosts generally follow the [Whitaker et al. \(2012\)](#) relation

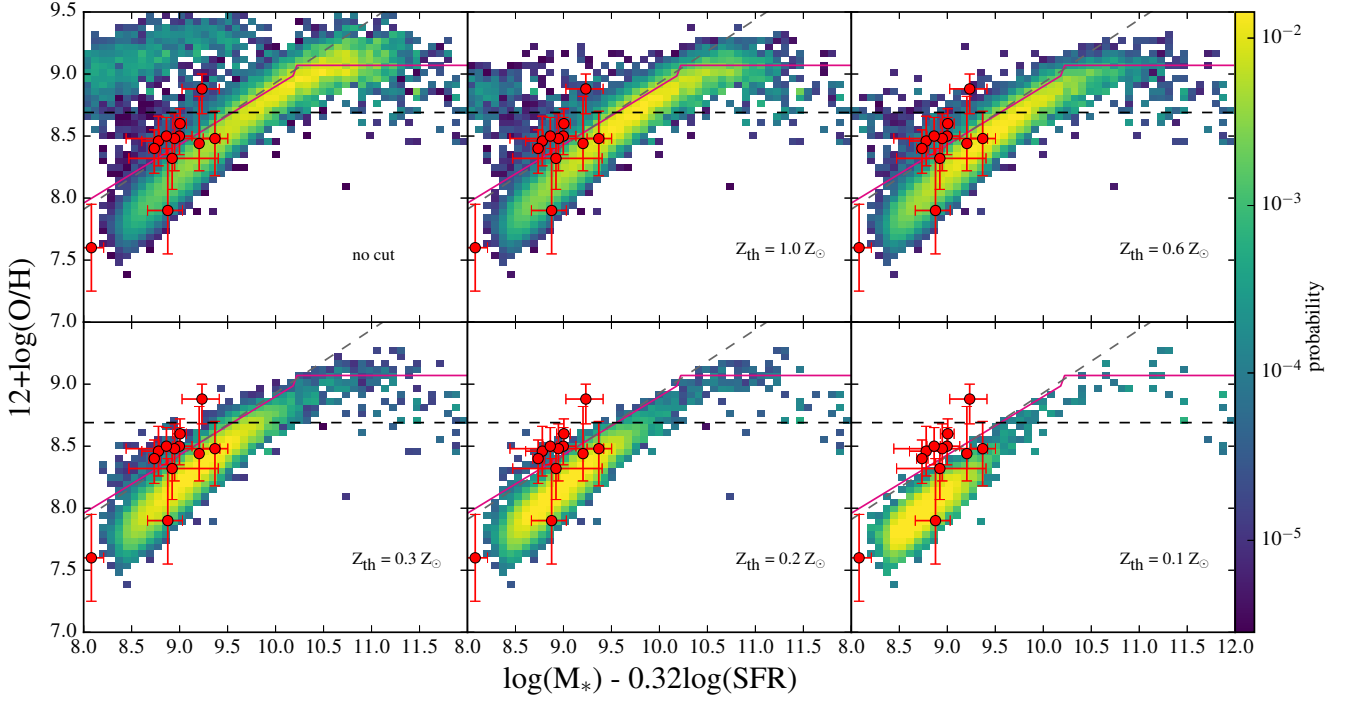


Figure 4. Fundamental metallicity relation of host galaxies in the Illustris simulation at $z = 0.7$. In each panel, the galaxies in each bin are weighted by the probability of hosting LGRBs for different metallicity thresholds. For comparison to observations, we show the BAT6 sample limited to $z < 1$ in the M08 calibration (red points). The FMR of field galaxies using the parametrised analytical models of Mannucci et al. (2010) (dashed lines) and Mannucci et al. (2011) (solid lines) are also shown.

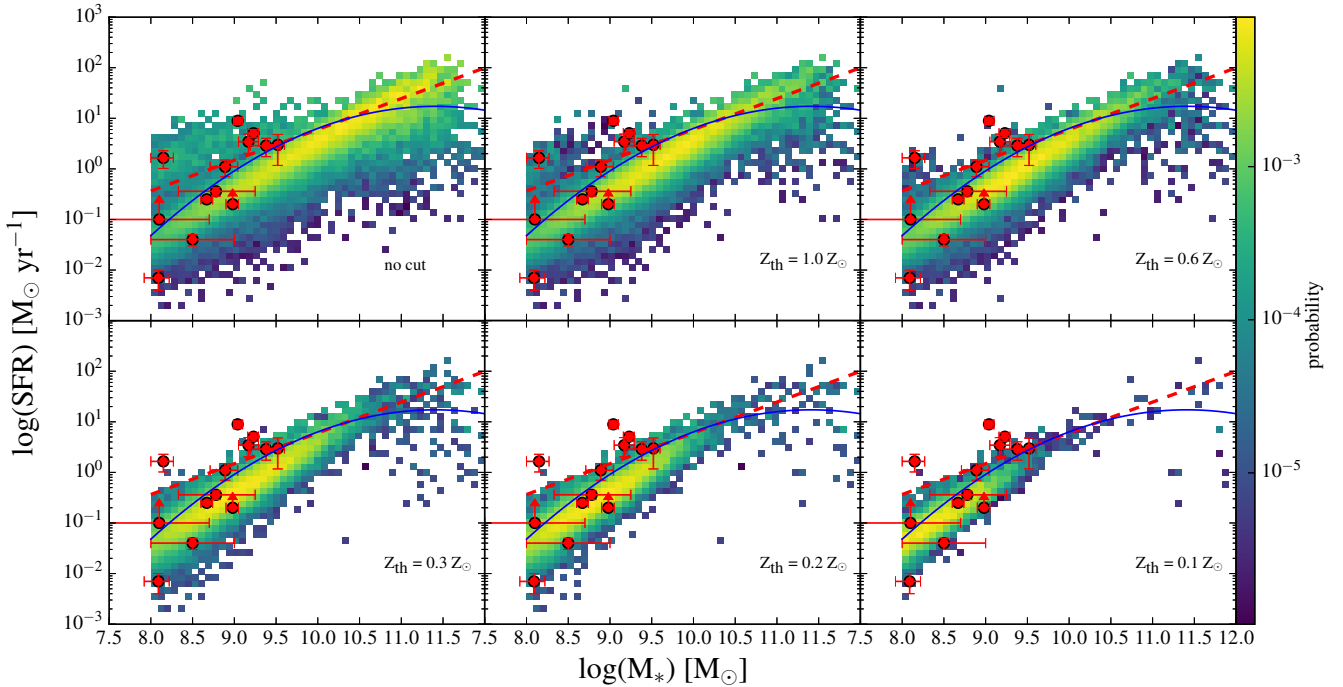


Figure 5. Star formation main sequence for host galaxies in the Illustris simulation at $z = 0.7$. In each panel the galaxies in a given bin are weighted by the probability of hosting LGRBs for different metallicity thresholds. For comparison, we show the Japelj et al. (2016) SFMS for the $z < 1$ BAT6 sample. The median relation derived by Whitaker et al. (2012, dashed red line) and Whitaker et al. (2014, solid blue line) are also displayed.

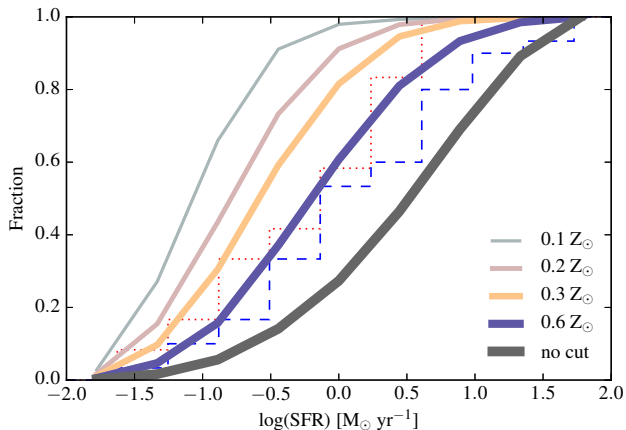


Figure 6. Cumulative SFR distribution of simulated LGRB hosts at $z = 0.7$, considering different metallicity thresholds. The BAT6 sample (dashed blue line) and the VLT/X-shooter sample (dotted red line) are included for comparison. Both observational samples are limited to $z < 1$.

with some scatter, the [Whitaker et al. \(2014\)](#) relation is an even better match, in agreement with the expected lower mass of LGRB hosts.

The Illustris simulation presents a clear SFMS that is in good agreement with observations at $z \sim 0$ and $z \sim 4$. However, the normalization of the SFMS is lower than observations at intermediate redshifts $z \sim 1$ and $z \sim 2$, as discussed in detail by [Genel et al. \(2014\)](#) and [Sparre et al. \(2015\)](#). The lower normalization of the SFMS is believed to be related to a broader peak in the Illustris $\dot{\rho}_{\text{SFR}}(z)$ ([Vogelsberger et al. 2014b](#)) and that the star formation and feedback processes are too closely linked to the dark matter evolution. Reproducing the evolution of the normalization is a challenge not only for the Illustris simulation but for theoretical models in general ([Davé 2008](#); [Damen et al. 2009](#)).

It is immediately clear from Fig. 5 that in the absence of a metallicity threshold, the simulated hosts determine a distribution extended towards higher SFRs than observations. We further examine this in Fig. 6 where we plot the normalized cumulative SFR distribution of the simulated galaxies at $z = 0.7$, compared to the BAT6 sample (dashed blue line) and the VLT/X-shooter sample (dotted red line), both limited to $z < 1$. Again, observational samples can be better matched by a $Z_{\text{th}} = 0.6 Z_{\odot}$ model than by the no-metallicity threshold model. We use a K-S test to quantify the agreement between observations and simulations, for $Z_{\text{th}} = 0.6 Z_{\odot}$ we obtained a p-value of 0.318 (0.110) for the BAT6 (VLT/X-shooter) sample. However, we note that an increase in the normalization of the SFMS would shift all simulated models to the right, leaving the $Z_{\text{th}} = 0.3$ model much closer to the observations.

It is important to point out that the MZR, FMR and now the SFMS of simulated LGRB hosts favour the same $Z_{\text{th}} = 0.6$ metallicity threshold. Also, in every case, resolving the apparent tensions in the properties of simulated galaxies compared to field galaxies would result in a shift towards a lower metallicity threshold (i.e. closer to $Z_{\text{th}} = 0.3$). All these relations are deeply correlated by star formation, chemical enrichment and feedback processes so it is encour-

aging to find that the behaviour of the simulated LGRB hosts is self-consistent.

The sSFR in Illustris inherits the normalization problems that originate in the SFMS. Additionally, at a given redshift, it becomes approximately independent of mass for $M_* < 10^{10.5} M_{\odot}$ which is at odds with observations by [Behroozi et al. \(2013\)](#) and [Whitaker et al. \(2012\)](#) (Fig. 7, first panel). The relation of [Whitaker et al. \(2014\)](#), on the other hand, does show a turn around of the sSFR at lower stellar masses which is more similar to the behaviour of the simulation. [Japelj et al. \(2016\)](#) studied the sSFR of the BAT6 sample and found that a significant fraction (27_{-9}^{+15} per cent) of hosts could be classified as starbursts according to their criteria. In Fig. 7 the LGRBs hosts appear to be equally scattered around the intrinsic sSFR of the simulation, for all metallicity thresholds considered. This suggests no preference for star-bursting LGRBs hosts in the Illustris simulation. This lack of starbursting hosts could be related to results by [Sparre et al. \(2015\)](#), who found a paucity of strong starbursts in the Illustris simulation presumably due to limited resolution that prevents tidal torques which drive starbursts during mergers. In this case, it is a caveat of the Illustris simulations and not a problem of the the LGRB model adopted in this work.

3.3.1 SFR redshift evolution

[Krühler et al. \(2015\)](#) found a clear evolution in the SFR of LGRB hosts with redshift. The observed median SFR of LGRB host increases from $\sim 0.6 M_{\odot} \text{ yr}^{-1}$ at $z \sim 0.5$ by a factor of 25 to $\sim 15 M_{\odot} \text{ yr}^{-1}$ at $z \sim 2$. For higher redshift only a weak evolution is observed, with the SFR levelling off at around $\sim 20 M_{\odot} \text{ yr}^{-1}$ at $z \sim 2$. In Fig. 8 we explore the evolution in SFR of Illustris LGRB hosts. To do so, we plot the mean SFR of LGRB hosts, for each metallicity threshold, as a function of redshift.

In order to properly compute the mean evolution of the SFR, a redshift dependent lower SFR limit that matches the average SFR sensitivity of the VLT/X-shooter sample (see figure 13 in [Krühler et al. 2015](#)) was considered. Compared to the VLT/X-shooter sample (blue triangles), all models present the same trend of increasing SFR with redshift up to $z \sim 3$, but only models with a metallicity threshold can match the low levels of SFR at low redshift. As shown in Fig. 8, the BAT6 sample for $z < 1$ (red dots) is also compatible with the VLT/X-shooter sample, reinforcing the previous conclusion.

4 INTERNAL METALLICITY DISPERSION

As pointed out in section 3.1, despite the paucity of high metallicity hosts, there is observational evidence of highly chemically enriched LGRB hosts, with metallicities larger than solar ([Graham et al. 2015](#)). This is also reproduced by the Illustris simulation, even when imposing a metallicity threshold for LGRB progenitors. This is possible because the ISM in a galaxy is not chemically homogeneous. The internal dispersion and variation of chemical abundances of the ISM are observationally proven in our Galaxy and in other galaxies (e.g. [Afferbach et al. 1997](#); [Smartt et al. 2001](#); [Sanders et al. 2012](#)). Hence, the metallicity of LGRB

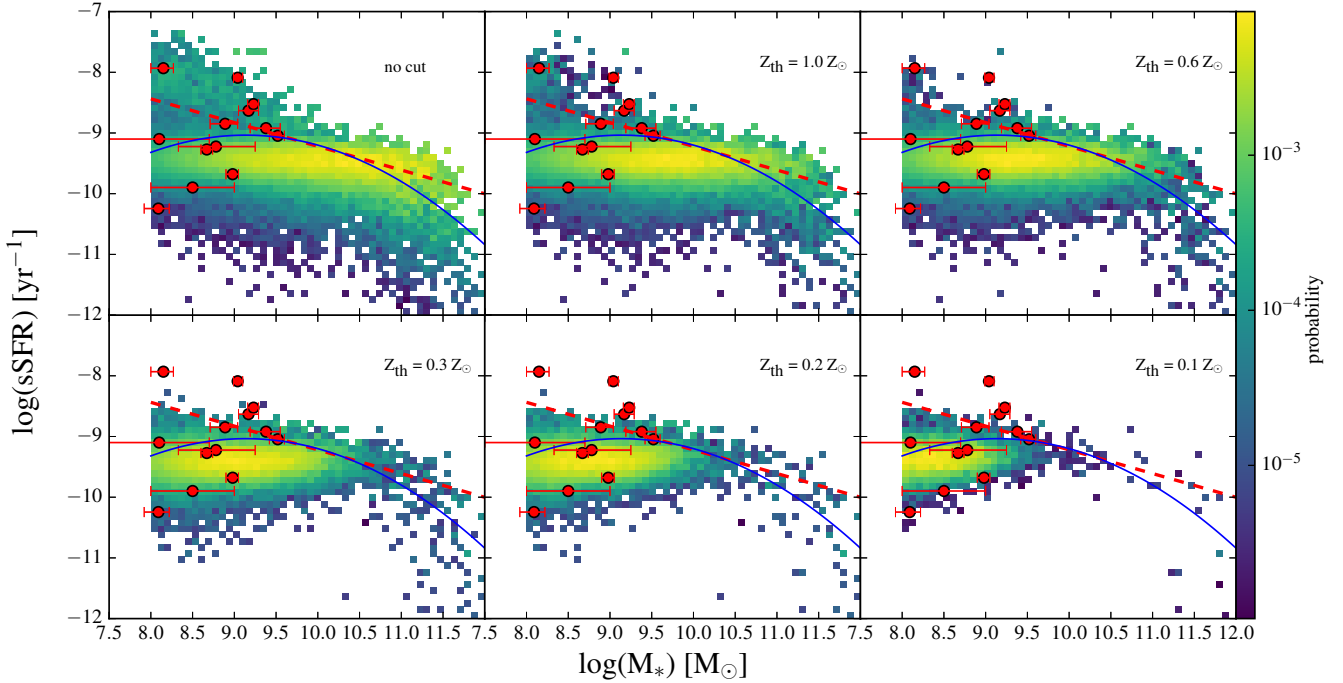


Figure 7. Specific star formation rate versus stellar mass for LGRB host galaxies in the Illustris simulation at $z = 0.7$. In each panel galaxies in a given bins are weighted by the probability of hosting an LGRB according to a different metallicity threshold. For comparison, the Japelj et al. (2016) SFMS for the BAT6 sample is included. The median relations derived by Whitaker et al. (2012, dashed red line) and Whitaker et al. (2014, dashed red line) are also shown.

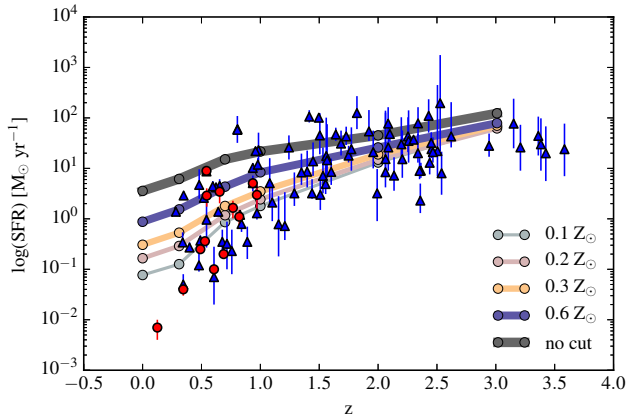


Figure 8. Evolution of the SFR of LGRB host galaxies as a function of redshift in the Illustris simulation for models with different Z_{th} (solid lines). The blue triangles represent the VLT/X-shooter sample. Red dots represent the BAT6 sample for $z < 1$.

progenitor sites might differ from the mean metallicity of the host galaxy.

Some tentative evidences of such effect has been reported for a small number of local galaxies, for which the LGRB region could be spatially-resolved (Christensen et al. 2008; Thöne et al. 2008; Levesque et al. 2011). They found that LGRB sites may indeed have slightly lower metallicities than the host average. However, more detailed studies remain challenging as the number of spatially-resolved hosts is very limited.

Metallicity gradients may also play an important role. Artale et al. (2011) found that scenarios favouring low-metallicity progenitors tend to produce LGRBs further out from the central regions than those allowing high metallicity progenitors at low z . However, some metallicity scatter is expected at each galactocentric radius, this scatter can be equal or even greater than the radial variation (Sanders et al. 2012). We therefore explore the role of metallicity dispersion (σ_z) in producing high metallicity hosts.

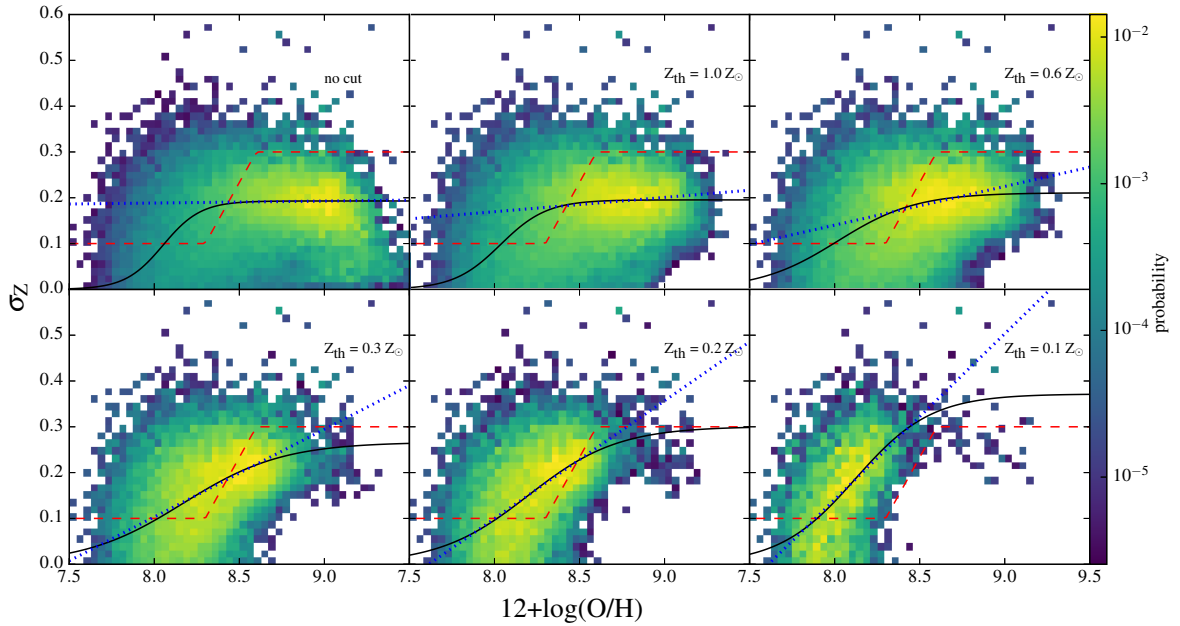
Niino et al. (2016) studied available LGRB hosts with $z < 0.41$. They compared the metallicity distribution to model predictions taking into account the spatial variation of metallicities among star forming regions within a galaxy. They found that models in which only low-metallicity stars ($12 + \log(\text{O}/\text{H}) < 8.2$) can trigger LGRBs reproduce the observed metallicity distribution. This is close to the value favoured by the Illustris simulation.

For our simulated LGRB host galaxies, it is possible to analyse the internal metallicity distribution in relation to the metallicity of the progenitor star. In Fig. 9 we show the internal metallicity dispersion as a function of the average host metallicity at $z = 0.3$. We choose to focus in a redshift range similar to that of the LGRB hosts studied by Niino et al. (2016). As can be seen, in the absence of a metallicity threshold, there is practically no correlation between the two quantities. But one does gradually appears when considering lower Z_{th} . We have quantified the correlation using a linear relation as well as a logistic curve. The latter matches the sigmoid appearance of the simulated results. The fitting parameters are presented in Table 1.

At $Z_{\text{th}} = 0.2 - 0.3Z_{\odot}$ the simulated metallicity dis-

Table 1. Best-fit parameter values for the $\sigma_Z - Z$ correlations in Fig. 9 corresponding to two possible parametrizations, a linear function given by $\sigma_Z = aZ + b$ and a logistic curve given by $\sigma_Z = c/(1 + \exp(-k(Z - d)))$

Z_{th}	a	b	c	d	k
no cut	$+0.004 \pm 0.008$	$+0.15 \pm 0.07$	$+0.19 \pm 0.001$	$+8.05 \pm 0.05$	$+9.01 \pm 2.64$
1.0	$+0.031 \pm 0.007$	-0.08 ± 0.07	$+0.20 \pm 0.002$	$+8.04 \pm 0.04$	$+7.32 \pm 1.49$
0.6	$+0.084 \pm 0.008$	-0.54 ± 0.07	$+0.21 \pm 0.005$	$+8.02 \pm 0.04$	$+4.33 \pm 0.79$
0.3	$+0.191 \pm 0.010$	-1.43 ± 0.09	$+0.27 \pm 0.022$	$+8.17 \pm 0.05$	$+3.43 \pm 0.60$
0.2	$+0.257 \pm 0.012$	-1.96 ± 0.1	$+0.3 \pm 0.034$	$+8.20 \pm 0.07$	$+3.79 \pm 0.60$
0.1	$+0.362 \pm 0.021$	-2.76 ± 0.17	$+0.37 \pm 0.062$	$+8.12 \pm 0.08$	$+4.48 \pm 0.71$

**Figure 9.** Internal metallicity dispersion of the host LGRBs galaxies in the Illustris simulation at $z = 0.3$ as a function of average galaxy metallicity. In each panel the bins are weighted by the probability of hosting an LGRB according to different metallicity thresholds. Solid (dotted) lines represent fits to the probability weighted maps assuming a logistic (linear) model. The red dashed line represents the internal metallicity dispersion model proposed by Niino et al. (2016).

persion largely agrees with that proposed by Niino et al. (2016). It is important to note that the correlation between metallicity and internal metallicity dispersion arises as a consequence of the metallicity threshold. This implies that, under the assumption of a stringent metallicity threshold ($Z_{\text{th}} = 0.1 - 0.3Z_{\odot}$), the simulation predicts that high metallicity hosts, which simultaneously have a high internal metallicity dispersion, are likely to be found.

In the case of models with $Z_{\text{th}} = 0.2 - 0.3Z_{\odot}$, the difference in σ_Z between low-metallicity hosts and high metallicity is not very large (~ 0.2 dex). This is in agreement with observations that show only a small decrease in the metal content of LGRB sites, compared to the average host metallicity. Also, by limiting the metallicity of the stellar progenitor instead of the metallicity of the host galaxy, our models favour a lower metallicity threshold in agreement with Niino et al. (2016). Other studies (Wolf & Podsiadlowski 2007; Kocovski et al. 2009; Perley et al. 2016b; Japelj et al.

2016) found instead a threshold closer to solar metallicity for efficient LGRB production.

5 MASS DISTRIBUTION

Beside low-metallicity and low-SFR, another feature of LGRB hosts is their low stellar mass at $z < 1$. Vergani et al. (2015) found that, in that redshift range, the BAT6 sample mass distribution was significantly shifted towards lower masses compared to galaxies in the UltraVISTA survey. Similarly, Perley et al. (2015) found a preference of LGRBs to occur in low stellar mass galaxies for a complete sample of radio-observed LGRB hosts.

Perley et al. (2016b) studied the rest-frame NIR luminosities and stellar masses of the SHOALS sample. They found a rapid increase in the NIR host luminosity between $z \sim 0.5$ and $z \sim 1.5$, and little variation for higher redshifts. In Fig. 10 we plot the cumulative stellar mass dis-

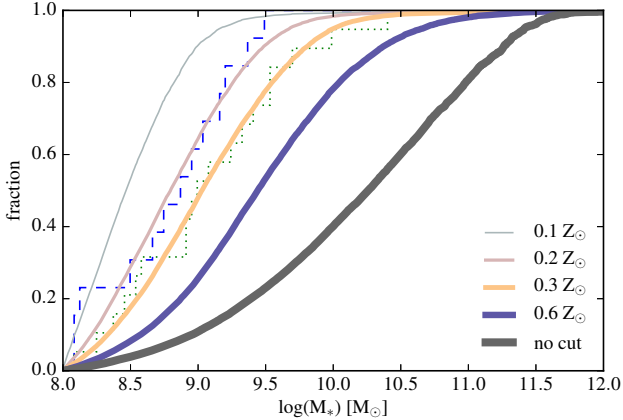


Figure 10. Cumulative mass distribution of simulated LGRB hosts at $z = 0.7$ for models with no metallicity threshold, as well as $Z_{\text{th}} = 0.1, 0.2, 0.3, 0.6 Z_{\odot}$. The blue dashed line represents the mass distribution of the BAT6 sample, while the green dotted line represents the SHOALS sample. Both observational samples are restricted to $z < 1$

tributions of the BAT6 and SHOALS sample at $z < 1$ together with the distribution of our simulated hosts considering different metallicity thresholds. Our results strongly discard that the observational samples could be drawn from the no metallicity threshold model. Compared to SHOALS, the BAT6 sample presents slightly lower stellar mass hosts and is better described by a $Z_{\text{th}} = 0.2 Z_{\odot}$ model (K-S test p-value=0.491), while the SHOALS sample is better described by a $Z_{\text{th}} = 0.3 Z_{\odot}$ model (K-S test p-value=0.606).

We remark that the metallicity threshold favoured by the simulation after analysing the stellar mass distribution ($Z_{\text{th}} \sim 0.3 Z_{\odot}$) is lower than what we found for the MZR, FMR and SFMS ($Z_{\text{th}} \sim 0.6 Z_{\odot}$). Unlike these latter relations, for which Illustris presents some departure from observed field galaxies, the stellar mass distribution of simulated galaxies is a close match to observations at all redshifts (Genel et al. 2014). Therefore, we point out that if the tensions in MZR and SFR between simulation and observations were resolved, the preferred threshold would be more in line to that found in this section ($Z_{\text{th}} \sim 0.3 Z_{\odot}$).

Vergani et al. (2015) also studied the effect of a metallicity bias on the stellar mass distribution of LGRB hosts. To do so, they applied a method similar to Campisi et al. (2009), using a galaxy catalogue constructed by combining high-resolution N-body simulations with a semi-analytic model of galaxy formation. Their results favoured a metallicity threshold $Z_{\text{th}} = 0.3 - 0.5 Z_{\odot}$, which is in agreement with the results found in previous sections, but is higher than what we find studying exclusively the stellar mass distribution.

Similarly, Perley et al. (2016b) proposed a simple model in which the LGRB efficiency is constant at low metallicity but falls sharply above a maximum metallicity threshold to explain the decrease of host stellar masses in the SHOALS sample at $z < 1.5$. They found a close to solar metallicity threshold, much higher than the value we find. Neither of the approaches taken by Vergani et al. (2015) and Perley et al. (2016b) took into account the internal metallicity dispersion of the galaxy, which would result in a lowering of the metallicity threshold in agreement with the results we show

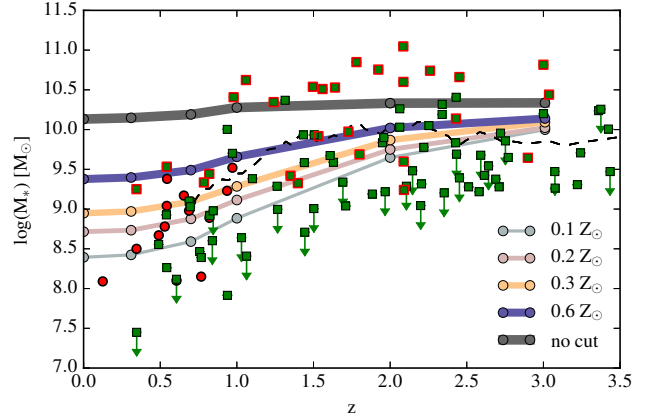


Figure 11. Evolution of the mean stellar mass of LGRB host as a function of redshift in the Illustris simulation under models with different Z_{th} (solid lines). The red dots represent the $z < 1$ BAT6 sample. Green squares represent the SHOALS sample. SHOALS hosts that present any evidence of dust obscuration are marked with an orange border. The dashed line represents the running mean of the SHOALS sample.

in the previous sections. It is therefore encouraging that further improvements in sub-grid physical models are likely to result in a better match of the present LGRB model to observations

We test whether the Illustris simulation is capable of reproducing the evolution of hosts stellar mass with redshift by computing the mean stellar mass as a function of redshift, weighted by the probability of hosting an LGRB assuming different metallicity thresholds. To compute the mean mass we assumed a redshift dependant lower mass limit that is compatible with the $m = 25$ NIR apparent magnitude detection limit of the SHOALS sample. The results are shown in Fig. 11 where we also display the SHOALS and BAT6 samples. We find that all models predict a mean host mass of $\sim 10^{10} M_{\odot}$ at $z = 3$. However, only models with a metallicity threshold can accurately reproduce the downsizing of LGRB host mass for lower redshift. Metallicity thresholds between $Z_{\text{th}} = 0.2 - 0.6 Z_{\odot}$ better reproduce the running mean of the SHOALS sample at lower redshift.

6 CONCLUSIONS

In this paper, we study the properties of LGRB host galaxies, comparing the latest observational hosts samples with a catalogue of simulated galaxies constructed from Illustris, a state-of-the-art hydrodynamical cosmological simulation. This kind of simulations, allows us to consider relevant processes for galaxy evolution, such as star formation and chemical enrichment, in a self consistent way. As well as to differentiate the properties of potential LGRB progenitors from the average properties of their host galaxies.

The aim of our investigation is to determine the validity of the metallicity dependant model. To do so we determine the probability of galaxies in the simulation to be considered hosting LGRBs under the assumption of the existence of selected metallicity thresholds: $Z_{\text{th}} = 0.1, 0.2, 0.3, 0.6, 1.0 Z_{\odot}$, as well as the null hypothesis of no metallicity dependence.

Our analysis shows that at $z < 1$, if no metallicity threshold is assumed, the MZR of simulated hosts is very different compared to the BAT6 sample, in particular, there is a large excess of simulated high-metallicity, high stellar mass hosts. We conclude from a more detailed study of the metallicity distribution, that BAT6 and VLT/X-Shooter observations are more consistent with a metallicity threshold in the range $Z_{\text{th}} = [0.3 - 0.6] Z_{\odot}$. We also find that the effect of the metallicity threshold in the MZR of hosts is basically to greatly reduce the probability of high-metallicity galaxies to hosts LGRBs. We find that lower metallicity hosts follow the intrinsic MZR of field galaxies in the simulation, with no apparent shift towards lower metallicities. This is in contrast to previous results based in semi-analytic simulations of galaxy formation (Campisi et al. 2011).

The fraction of simulated LGRB hosts with metallicities above solar is ~ 25 percent under the assumption of models with $Z_{\text{th}} = 0.6 Z_{\odot}$. This value is comparable to the fractions of high metallicity hosts found in observational samples, in particular the 24 ± 10 per cent of supra-solar metallicity hosts in the VLT/X-Shooter found by Krühler et al. (2015) and the 16_{-8}^{+16} percent found by Japelj et al. (2016) for the BAT6 sample.

Metallicity dispersion plays an important role in the presence of highly enriched LGRB hosts. We find that, if a $Z_{\text{th}} \sim 0.6 Z_{\odot}$ threshold is assumed, then high metallicity hosts also exhibit a larger internal metallicity dispersion. We have quantified the correlation between internal metallicity dispersion and averaged host metallicity using fits to a linear and logistic models. We also notice that the internal metallicity dispersion of hosts assuming $Z_{\text{th}} = 0.3 - 0.2 Z_{\odot}$ predicted by Illustris roughly matches the model proposed by Niino et al. (2016) to explained the properties of $z < 0.4$ LGRB hosts.

The FMR of simulated hosts presents a similar behaviour than the MZR. Host galaxies follow the intrinsic FMR of simulated galaxies, with the effect of a metallicity threshold being to make lower metallicity galaxies the more likely hosts. Again, we find a better match to observations for thresholds in the $Z_{\text{th}} = [0.3 - 0.6] Z_{\odot}$ range. Therefore, we conclude that at low redshift simulated LGRB hosts follow both the FMR and MZR simultaneously, but with a paucity of high-metallicity hosts, in accordance with observational results by Japelj et al. (e.g. 2016).

From studying the SFMS of LGRB hosts we find that in the absence of a metallicity threshold, the star formation of LGRB hosts at $z \sim 1$ extends towards much higher SFRs than in the BAT6 and VLT/X-shooter samples. Observations are better matched by a $Z_{\text{th}} = 0.6 Z_{\odot}$ threshold, but given that the SFMS of the Illustris simulation presents generally a lower normalization than observed galaxies, a lower threshold $Z_{\text{th}} = 0.3 Z_{\odot}$ is possible. We also find that the Illustris simulation reproduces the evolution of the SFR of LGRB hosts with redshift in the VLT/X-shooter sample when a metallicity threshold is assumed. Under all conditions, simulated hosts increase their average SFR with redshift up to $z = 3$, but only models with a strong metallicity threshold reproduce the lower SFRs of low redshift hosts.

Finally, the stellar mass distribution of LGRB hosts at $z < 1$ cannot be reproduced by Illustris without a metallicity threshold. The stellar mass distribution of the SHOALS sample is best described by a metallicity thresh-

old $Z_{\text{th}} = 0.3 Z_{\odot}$, while the BAT6 sample is better described by a lower value of $Z_{\text{th}} = 0.2 Z_{\odot}$. We notice that this thresholds are much lower than the close to solar metallicity values estimated by Japelj et al. (2016) for the BAT6 sample and Perley et al. (2016b) for the SHOALS sample. Thanks to the nature of the hydrodynamical simulation, we are able to easily differentiate between the metallicity of LGRB progenitors and the metallicity of LGRB hosts and take into account the internal metallicity dispersion of galaxies seamlessly, this results in lower metallicity threshold that is closer to what is expected under the collapsar progenitor model. We also find that models with $Z_{\text{th}} = 0.3 - 0.6 Z_{\odot}$, correctly predict the increase in stellar mass with redshift of LGRB host present in the SHOALS sample.

Illustris provides us with the largest sample of simulated well-resolved LGRB hosts so far analysed. Certainly, there is still room for improvement of subgrid models, specially those related to feedback and chemical enrichment, but globally, the simulation is able to reproduce a large number of key LGRB host properties, their MZR, FMR, SFR and stellar mass. The internal metallicity dispersion of galaxies seems to be crucial to understand the origin of LGRBs and their relation with their host galaxies. All the results support the existence of a metallicity threshold in the order $Z_{\text{th}} = 0.3 - 0.6 Z_{\odot}$, which is lower than some of the estimations reported by previous works.

ACKNOWLEDGEMENTS

The authors acknowledge the grants PICT 2011-0959 from Argentinian ANPCyT, and PIP 2012-0396 from Argentinian CONICET and Fondecyt Regular 115033, Southern Astro-physics Network Redes Conicyt 150078 and proyecto interno MUN UNAB 2015. This research made use of Astropy (Astropy Collaboration et al. 2013), numpy (Walt et al. 2011), and matplotlib (Hunter 2007).

REFERENCES

- Afflerbach A., Churchwell E., Werner M. W., 1997, *ApJ*, 478, 190
 Alloin D., Collin-Souffrin S., Joly M., Vigroux L., 1979, *A&A*, 78, 200
 Artale M. C., Pellizza L. J., Tissera P. B., 2011, *MNRAS*, 415, 3417
 Asplund M., Grevesse N., Sauval A. J., Scott P., 2009, *ARA&A*, 47, 481
 Astropy Collaboration et al., 2013, *A&A*, 558, A33
 Basa S., Cuby J. G., Savaglio S., Boissier S., Clément B., Flores H., Le Borgne D., Mazure A., 2012, *A&A*, 542, A103
 Behroozi P. S., Wechsler R. H., Conroy C., 2013, *ApJ*, 770, 57
 Brinchmann J., Charlot S., White S. D. M., Tremonti C., Kauffmann G., Heckman T., Brinkmann J., 2004, *MNRAS*, 351, 1151
 Campisi M. A., De Lucia G., Li L.-X., Mao S., Kang X., 2009, *MNRAS*, 400, 1613
 Campisi M. A., Tapparello C., Salvaterra R., Mannucci F., Colpi M., 2011, *MNRAS*, 417, 1013
 Chabrier G., 2003, *PASP*, 115, 763
 Chisari N. E., Tissera P. B., Pellizza L. J., 2010, *MNRAS*, 408, 647
 Christensen L., Vreeswijk P. M., Sollerman J., Thöne C. C., Le Floc’h E., Wiersema K., 2008, *A&A*, 490, 45

- Courty S., Björnsson G., Gudmundsson E. H., 2004, *MNRAS*, 354, 581
- Curti M., Cresci G., Mannucci F., Marconi A., Maiolino R., Esposito S., 2017, *MNRAS*, 465, 1384
- Daddi E., et al., 2007, *ApJ*, 670, 156
- Damen M., et al., 2009, *ApJ*, 705, 617
- Davé R., 2008, *MNRAS*, 385, 147
- Davis M., Efstathiou G., Frenk C. S., White S. D. M., 1985, *ApJ*, 292, 371
- Dolag K., Borgani S., Murante G., Springel V., 2009, *MNRAS*, 399, 497
- Dopita M. A., Kewley L. J., Sutherland R. S., Nicholls D. C., 2016, *Ap&SS*, 361, 61
- Fruchter A. S., et al., 2006, *Nature*, 441, 463
- Fryer C. L., Heger A., 2005, *ApJ*, 623, 302
- Fynbo J. P. U., et al., 2009, *ApJS*, 185, 526
- Genel S., et al., 2014, *MNRAS*, 445, 175
- Graham J. F., Fruchter A. S., 2013, *ApJ*, 774, 119
- Graham J. F., et al., 2015, arXiv:1511.00667 [astro-ph]
- Greiner J., et al., 2015, *ApJ*, 809, 76
- Heuvel V. D., J E. P., Zwart P., F S., 2013, *ApJ*, 779, 114
- Hinshaw G., et al., 2013, *ApJS*, 208, 19
- Hjorth J., et al., 2003, *Nature*, 423, 847
- Hjorth J., et al., 2012, *ApJ*, 756, 187
- Hunt L. K., et al., 2014, *A&A*, 565, A112
- Hunter J. D., 2007, *CS&E*, 9, 90
- Izzard R. G., Ramirez-Ruiz E., Tout C. A., 2004, *MNRAS*, 348, 1215
- Japelj J., et al., 2016, *A&A*, 590, A129
- Jimenez R., Piran T., 2013, *ApJ*, 773, 126
- Katz N., Gunn J. E., 1991, *ApJ*, 377, 365
- Kewley L. J., Ellison S. L., 2008, *ApJ*, 681, 1183
- Kistler M. D., Yüksel H., Beacom J. F., Stanek K. Z., 2008, *ApJ*, 673, L119
- Kobulnicky H. A., Kewley L. J., 2004, *ApJ*, 617, 240
- Kocevski D., West A. A., Modjaz M., 2009, *ApJ*, 702, 377
- Krühler T., et al., 2015, *A&A*, 581, A125
- Lapi A., Kawakatu N., Bosnjak Z., Celotti A., Bressan A., Granato G. L., Danese L., 2008, *MNRAS*, 386, 608
- Le Floc'h E., et al., 2003, *A&A*, 400, 499
- Levesque E. M., Kewley L. J., Graham J. F., Fruchter A. S., 2010, *ApJ Letters*, 712, L26
- Levesque E. M., Berger E., Soderberg A. M., Chornock R., 2011, *ApJ*, 739, 23
- MacFadyen A. I., Woosley S. E., 1999, *ApJ*, 524, 262
- Maiolino R., et al., 2008, *A&A*, 488, 463
- Mannucci F., Cresci G., Maiolino R., Marconi A., Gnerucci A., 2010, *MNRAS*, 408, 2115
- Mannucci F., Salvaterra R., Campisi M. A., 2011, *MNRAS*, 414, 1263
- Marinacci F., Pakmor R., Springel V., Simpson C. M., 2014, *MNRAS*, 442, 3745
- McGaugh S. S., 1991, *ApJ*, 380, 140
- Modjaz M., et al., 2008, *Aj*, 135, 1136
- Mosconi M. B., Tissera P. B., Lambas D. G., Cora S. A., 2001, *MNRAS*, 325, 34
- Moustakas J., Kennicutt R. C., Tremonti C. A., Dale D. A., Smith J.-D. T., Calzetti D., 2010, *ApJS*, 190, 233
- Navarro J. F., White S. D. M., 1993, *MNRAS*, 265, 271
- Niino Y., 2011, *MNRAS*, 417, 567
- Niino Y., et al., 2016, LPI Contributions, 1962, 4039
- Nuza S. E., Tissera P. B., Pellizza L. J., Lambas D. G., Scannapieco C., de Rossi M. E., 2007, *MNRAS*, 375, 665
- Pagel B. E. J., Edmunds M. G., Blackwell D. E., Chun M. S., Smith G., 1979, *MNRAS*, 189, 95
- Perley D. A., et al., 2013, *ApJ*, 778, 128
- Perley D. A., et al., 2015, *ApJ*, 801, 102
- Perley D. A., et al., 2016a, *ApJ*, 817, 7
- Perley D. A., et al., 2016b, *ApJ*, 817, 8
- Pettini M., Pagel B. E. J., 2004, *MNRAS*, 348, L59
- Pilyugin L. S., Grebel E. K., 2016, *MNRAS*, 457, 3678
- Podsiadlowski P., Ivanova N., Justham S., Rappaport S., 2010, *MNRAS*, 406, 840
- Robertson B. E., Ellis R. S., 2012, *ApJ*, 744, 95
- Salim S., et al., 2007, *ApJS*, 173, 267
- Salvaterra R., 2015, *JHEAp*, 7
- Salvaterra R., et al., 2012, *ApJ*, 749, 68
- Salvaterra R., Maio U., Ciardi B., Campisi M. A., 2013, *MNRAS*, 429, 2718
- Sanders N. E., Caldwell N., McDowell J., Harding P., 2012, *ApJ*, 758
- Savaglio S., Glazebrook K., Le Borgne D., 2009, *ApJ*, 691, 182
- Scannapieco C., Tissera P. B., White S. D. M., Springel V., 2005, *MNRAS*, 364, 552
- Scannapieco C., Tissera P. B., White S. D. M., Springel V., 2006, *MNRAS*, 371, 1125
- Schulze S., et al., 2015, *ApJ*, 808, 73
- Smartt S. J., Venn K. A., Dufton P. L., Lennon D. J., Rolleston W. R. J., Keenan F. P., 2001, *A&A*, 367, 86
- Sparre M., et al., 2015, *MNRAS*, 447, 3548
- Springel V., 2010, *MNRAS*, 401, 791
- Springel V., Hernquist L., 2003, *MNRAS*, 339, 289
- Springel V., White S. D. M., Tormen G., Kauffmann G., 2001, *MNRAS*, 328, 726
- Stanek K. Z., et al., 2006, *Acta Astronomica*, 56, 333
- Svensson K. M., Levan A. J., Tanvir N. R., Fruchter A. S., Strolger L.-G., 2010, *MNRAS*, 405, 57
- Tanvir N. R., et al., 2012, *ApJ*, 754, 46
- Thöne C. C., et al., 2008, *ApJ*, 676, 1151
- Torrey P., Vogelsberger M., Genel S., Sijacki D., Springel V., Hernquist L., 2014, *MNRAS*, 438, 1985
- Trenti M., Perna R., Jimenez R., 2015, *ApJ*, 802, 103
- Vergani S. D., et al., 2015, *A&A*, 581, A102
- Vogelsberger M., Genel S., Sijacki D., Torrey P., Springel V., Hernquist L., 2013, *MNRAS*, 436, 3031
- Vogelsberger M., et al., 2014a, *MNRAS*, 444, 1518
- Vogelsberger M., et al., 2014b, *Nature*, 509, 177
- Walt S. v. d., Colbert S. C., Varoquaux G., 2011, *CS&E*, 13, 22
- Whitaker K. E., van Dokkum P. G., Brammer G., Franx M., 2012, *ApJ*, 754, L29
- Whitaker K. E., et al., 2014, *ApJ*, 795, 104
- Wiersma R. P. C., Schaye J., Theuns T., Dalla Vecchia C., Tornatore L., 2009, *MNRAS*, 399
- Wolf C., Podsiadlowski P., 2007, *MNRAS*, 375, 1049
- Woosley S. E., 1993, *ApJ*, 405, 273
- Woosley S. E., Heger A., 2006, *ApJ*, 637, 914

This paper has been typeset from a $\text{\TeX}/\text{\LaTeX}$ file prepared by the author.